

## X-ray binaries

H. SCHATZ <sup>a</sup> and K. E. REHM <sup>b</sup>

<sup>a</sup>National Superconducting Cyclotron Laboratory  
Dept. of Physics and Astronomy  
Joint Institute for Nuclear Astrophysics  
Michigan State University  
East Lansing, MI 48824

<sup>b</sup>Physics Division  
Argonne National Laboratory

### 1. Introduction

X-ray binaries are among the brightest extra-solar objects in the sky and are characterized by dramatic variabilities in brightness on timescales ranging from milliseconds to months and years. Their main source of power is the gravitational energy released by matter accreted from a companion star and falling onto a neutron star or a black hole in a close binary system. X-ray binaries therefore serve as rich sources of information about compact stellar objects, and, once understood, could be used as unique natural laboratories for the properties of matter under extreme conditions.

In recent years, the launching of a number of X-ray observatories has marked the beginning of a new era in X-ray astronomy. These include Beppo SAX, RXTE, Chandra X-ray observatory and XMM-Newton. These facilities provide(d) unprecedented sensitivity, all-sky coverage, and timing resolution and led to a range of new discoveries related to X-ray binaries, such as ms-oscillations, superbursts, and quiescent luminosity measurements in transients. Similar advances in the underlying nuclear physics are now needed to make full use of these observations towards a better understanding of the physics of X-ray binaries, and to solve the many open questions. In this review we concentrate on accreting neutron star systems, where observables are to a large extent governed by nuclear physics. For some recent reviews see Psaltis 2004 [1] or Strohmayer & Bildsten 2003 [2].

In section 2 we summarize recent observational results, open questions, and their relation to the underlying nuclear physics. In section 3 we summarize the current status of the nuclear physics, identify the major uncertainties, and give an outlook on the role that future radioactive beam facilities such as RIA can play in this field.

### 2. Nuclear processes and their observables

A fluid element consisting of hydrogen and helium that is accreted onto the surface of a neutron star is continuously compressed by the matter accumulating on top of it.

Eventually the element will become part of the liquid ocean and later of the solid crust of the neutron star. The thin outer crust of a neutron star represents just  $\approx 10^{-4}M_{\odot}$  of material. At typical accretion rates of  $10^{-8}$ - $10^{-10}M_{\odot}/\text{yr}$  this material is therefore replaced after about  $10^4$ - $10^6$  years of accretion. This is short compared to the duration of the mass transfer phase in low mass X-ray binaries. Therefore the majority of neutron stars in low mass X-ray binaries should have an accreted crust.

On its journey into the neutron star interior the accreted fluid element undergoes a sequence of nuclear processes converting hydrogen and helium into exotic nuclei ranging from the proton drip line during X-ray bursts to the neutron drip line upon entering the inner crust. These processes together with their relation to observations and current open questions are discussed in the following subsections in the order they occur. The ashes of each process form the initial composition for the next, and the energy release of a nuclear process deep in the crust sets the thermal environment for the surface processes. Therefore, all processes are connected and need to be understood in a selfconsistent way.

### 2.1. Spectral features and spallation of metals

During the 10-100 s of an X-ray burst (see Sec. 2.2) the X-ray flux is dominated by thermal emission from the dramatically heated neutron star photosphere. This offers the opportunity to obtain compositional information from absorption features in the X-ray spectrum. In addition, observed spectral features allow one to determine the gravitational redshift on the neutron star surface and therefore the compactness (mass/radius) of the neutron star.

Some observations of a  $\approx 4$  keV absorption feature have been reported over the last 20 years for various systems (see recent review in Bildsten, Chang, and Paerels 2003 [3]). More recently, Cottam, Paerels, and Mendez 2002 [4], reported the detection of hydrogen and helium like Fe absorption lines and derive a redshift of  $Z = 0.35$  for the neutron star in EXO 0748-676. This has provided an important constraint for the neutron star mass radius relation and the nuclear equation of state. In addition a recently discovered 45 Hz oscillation during an X-ray burst [6] in EXO 0748-676 has been associated with the spin frequency of the underlying neutron star (see Sec. 2.2). The neutron star in EXO 0748-676 apparently rotates much slower than other neutron stars in X-ray bursters that typically spin with frequencies ranging from 270 to 620 Hz [2]. The reduced rotational line broadening in EXO 0748-676 might be the reason why a spectral line could be detected in this system. The known spin frequency also offers the opportunity to use precise modeling of the spectral line shapes to constrain the neutron star radius and therefore the dense matter equation of state.

As Joss 1977 [7] pointed out, the large entropy difference between the deeper layers that undergo explosive hydrogen and helium burning during X-ray bursts (2.2) and the photosphere prevents in principle convection from transporting burst ashes to the surface (see however Weinberg, Bildsten, and Schatz 2006 [8] for exceptions related to photospheric radius expansion bursts). On the other hand, heavy elements such as Fe entering the photosphere via accretion, sink within seconds beneath the photosphere owing to the strong gravity on the neutron star surface [3]. Elemental abundance observations in the neutron star photosphere during X-ray bursts therefore probe directly the ongoing accretion and provide information on the accreted composition as well as the trajectories of

the infalling matter. In particular, infall under steep angles can lead to the spallation of heavy elements [5] contained in the accretion flow. This has been investigated in detail by Bildsten, Chang, and Paerels 2003 [3], who follow the cascade of fragmentation processes and predict the final abundances. They find, that the amount of iron that can be present in the photosphere is about a factor of 20 short of explaining the observed line strength, but argue for more accurate studies before drawing definite conclusions.

Spallation of heavy elements is also important for X-ray burst calculations. The abundance of CNO elements entering the deeper atmosphere of the neutron star controls how much hydrogen can be burned away by the CNO cycle prior to the triggering of an X-ray burst.

## 2.2. X-ray bursts and the rp-process

Shortly after the discovery of X-ray bursts in 1976 [9,10] they were correctly interpreted as thermonuclear explosions on the surface of an accreting neutron star [11,12,7,13]. Hydrogen or helium-rich matter from the envelope of the companion star accumulates on the neutron star for hours to days. Eventually the ignition of extremely temperature sensitive fusion reactions leads to the thin shell instability of Hansen and VanHorn 1975 [14], where the heating from thermonuclear reactions cannot be compensated by readjusting the stellar structure or cooling through the surface. The result is a thermonuclear runaway where rising temperatures accelerate the thermonuclear reaction rates leading to more rapid temperature rises, still faster thermonuclear reactions and so on. The resulting thermonuclear energy release lasts 10-100 s and can be directly observed as an X-ray outburst of typically  $10^{39-40}$  ergs. Burst recurrence times are of the order of hours to days and long sequences of burst can be observed. About 60 galactic X-ray bursting systems are known today making X-ray bursts a frequent phenomenon in our Galaxy (see [1,15,16] for reviews on observations and physics of X-ray bursts).

Over the last years a dramatic increase in observational data has led to a large database of burst properties monitored over long periods of time, and has also led to new discoveries such as ms oscillations of the X-ray flux during X-ray bursts [17,2]. These oscillations have been interpreted as anisotropies in the nuclear burning on the surface of the rapidly rotating neutron star, caused for example by a spreading hot spot. In this model the slight frequency changes observed over the burst duration are explained by the rotational decoupling of the surface layer that slows down during the burst driven expansion of the neutron star atmosphere and then reaccelerates during the following cooling and contraction. However, in some cases the frequency changes of the oscillations are too large to be explained with a rotationally decoupled layer [18]. Alternative explanations for the frequency drifts include various surface oscillation modes [19,20,21]. The frequencies of these modes depend on the composition and therefore on the nuclear physics of X-ray bursts. In any case, the recent observations of ms oscillations during X-ray bursts in the two known X-ray bursting pulsars, SAX J1808.4-3658 [22] and XTE J1814-338 [23], where the spin frequency is known from the regular pulsations, have finally proven the relationship between burst oscillations and neutron star spin.

Observations of ms oscillations are important for many reasons. First they allow to experimentally explore the X-ray burst behavior and the underlying nuclear processes as a function of neutron star spin [24]. Second, as Strohmayer 2004 [25] pointed out

gravitational light bending effects in principle would allow one to extract mass and radius of the neutron star together with the time-dependent size of the surface burning area from a detailed analysis of pulse trains. Already first constraints on the mass radius relationship of the neutron star in XTE J1814-338 have been obtained with this method [26].

The nuclear processes powering X-ray bursts and the related observational features depend strongly on the system parameters, such as mass accretion rate, accreted abundances of hydrogen, helium, and CNO metals, rotation, and the thermal flux at the surface originating from nuclear reactions deep in the crust [15].

Most systems have mass accretion rates in excess of  $4.4 \times 10^{-10} M_{\odot}/yr$  and accrete a mix of hydrogen, helium and some heavy metals most likely in solar proportions. In this case, the burst is triggered by the temperature sensitivity of helium burning via the  $3\alpha$  reaction, igniting helium in a hydrogen rich surface layer [15]. The helium ignition triggers hydrogen burning via the rapid proton capture process (rp-process) [28,29,30] and peak temperatures of 1-2 GK are reached.

Because of the factor of 10 larger energy release per nucleon, hydrogen burning via the rp-process is the main energy source for X-ray bursts and determines the X-ray light curve. Nevertheless, because of its computational demanding nature, the full rp-process has only been recently included in X-ray burst calculations, opening the door for quantitative comparisons with observations. In a first step, Schatz et al. 2001 [31] included the full rp-process in a one-zone model after exploratory studies with smaller networks [30,32]. This led to the discovery of a SnSbTe cycle which is formed by  $(\gamma, \alpha)$  reactions on  $\alpha$ -unbound proton-rich Te isotopes. The resulting rp-process path is shown in Fig. 1 for an X-ray burst where large amounts of hydrogen are available at burst ignition. The SnSbTe cycle represents a natural end point for any single outburst rp-process. In principle heavier elements could be produced in a multi-burst rp-process where the heavy ashes decay back to stability and are then again irradiated with protons thereby bypassing the Sn-Sb-Te cycle [33]. So far there is no plausible astrophysical scenario known where this would occur.

Besides delineating the full rp-process path for the first time, three main conclusions were drawn from these one-zone calculations. First, hydrogen is always burned completely making the occurrence of deep hydrogen burning via electron capture [34] unlikely. Second, the rp-process beyond Fe includes particularly long-lived  $\beta$ -decays at  $^{64}\text{Ge}$ ,  $^{68}\text{Se}$ ,  $^{72}\text{Kr}$  and  $^{104}\text{Sn}$  (so-called waiting points) that slow the process down and extend the energy release of the burst considerably. The result is an increase of the burst duration from a few 10 s of seconds to 100-300 s. Qualitatively similar conclusions have been drawn by Koike et al. 1999 [35] based on a similar one-zone model but with a more limited reaction network. As a consequence, the observation of long X-ray bursts with durations of the order of 100 s can now be used as an indicator for mixed hydrogen and helium burning providing a powerful constraint for models and system parameters. The third conclusion drawn from one-zone X-ray burst calculations is that the long-lived waiting points along the rp-process path lead to a wide spread of the final abundance distribution [31,36]. Therefore the crust of an accreting neutron star is characterized by a very impure lattice structure that strongly affects crust properties such as thermal and electrical conductivities (see Sec. 2.4). Koike et al. 2004 [37] obtain similar results by combining

a full one-dimensional X-ray burst multizone model with a very limited nuclear reaction network to calculate temperature and density conditions followed by postprocessing with a full reaction network. However, it has been shown that even at late stages of the burst nuclear reactions on heavier nuclei beyond iron produce significant amounts of energy and can still determine temperature and observed light curves [35,31]. Therefore, for X-ray bursts postprocessing does not reproduce the correct conditions and nuclear reaction flows (see also [38] for an example).

More recently the first one-dimensional multizone calculations of a sequence of X-ray bursts have been performed with the full rp-process [27,39]. These calculations confirmed the main conclusions from the earlier one-zone models, but also yielded some important differences. Most importantly, the ignition conditions for bursts late in the burst sequence change because of the presence of partially burned ashes from preceding bursts. This is the well known compositional inertia effect already pointed out by Taam (1980) [43]. The main consequence is increased hydrogen burning between bursts leaving less hydrogen for the X-ray bursts itself. Nevertheless, bursts at high accretion rates still burn enough hydrogen for the rp-process to reach the first long-lived waiting points in the  $A = 64$  region and therefore still lead to long duration X-ray bursts. For the few system parameters explored so far the SnSbTe cycle is only reached in the very first burst after the onset of accretion. This is of potential interest for transient systems, where the observation of the sequence of bursts after the accretion turns on could provide important constraints for X-ray burst models and the structure of the underlying neutron star. In the system Acq X-1 such a first burst might have been observed [40], and its unusual long duration would be consistent with a particularly extended phase of hydrogen burning [41]

A first quantitative comparison of calculated burst profiles from the one-dimensional model of Woosley et al. [27] with the so-called "textbook" burster GS 1826-24 has yielded excellent agreement [42] for certain choices in the nuclear physics. GS 1826-24 exhibits extremely regular bursts with a period of 3-6 hours and observation over many years has yielded very accurate burst profiles. Galloway et al. 2004 [44] in fact find a slight change in burst profile from observations in the years 1998 and 1999 to observations in the year 2000 due to a slight increase in accretion rate. It remains to be seen whether these changes can be reproduced in current models, but observations like this certainly provide unprecedented quantitative tests for X-ray burst models. However, the nuclear physics of the rp-process is far from being sufficiently accurate to test X-ray burst models at this level. This has been clearly demonstrated with studies of the sensitivity of calculated X-ray burst light curves to uncertainties in masses around the major waiting points  $^{64}\text{Ge}$ ,  $^{68}\text{Se}$ , and  $^{72}\text{Kr}$  in a one-zone model [98]. More recent studies with multi-zone X-ray burst models predicting light curves for various changes in  $\beta$ -decay half-lives, which were intended to simulate mass uncertainties, come to similar conclusions [27]. It is likely that these studies rather underestimate the nuclear physics uncertainties in predicted X-ray burst light curves as there are additional, large uncertainties in nuclear reaction rates (see Sec. 3). Clearly, the current status of the nuclear physics of the rp-process does not allow full interpretation of X-ray observations in a quantitative way. The success of modeling the burst profiles of GS 1826-24 is promising but does therefore not necessarily imply that current astrophysical models and their parameter choices are correct.

There are many other open questions related to the nuclear burning in X-ray bursts.

For example, the ignition and subsequent burning front propagation across the neutron star surface is not understood. This relates directly to the observations of ms oscillations during bursts which could originate from unisotropic burning across the rapidly spinning neutron star surface when the accreted layer ignites at one, or a few spots or patches. First attempts with analytical considerations or simplified models have been made to investigate the spreading of a burning front across the neutron star surface [45,46,47]. They find that the burning front is most likely a deflagration front driven by convection. As Zingale et al. [48] point out a localized ignition does not seem possible, at least when neglecting rotation. It would be desirable to explore this in full 2D or 3D hydrodynamic calculations. Such calculations have so far only been done for the first 150  $\mu\text{s}$  in the much easier case of a pure He detonation [49].

Another major problem in understanding X-ray bursts is the dramatic change in bursting behavior once the accretion rate exceeds about  $0.13 \dot{M}_{\text{Edd}}$ . Current simple X-ray burst models predict that with increasing accretion rate ignition conditions are reached earlier leading to more frequent bursts. At the same time the burst duration should become longer as there is less time to burn hydrogen during the accretion phase leaving more fuel for the slow rp-process in bursts. While this behavior is qualitatively confirmed for the slight change of accretion rate in the textbook burster GS 1826-24 [27], the observed behavior beyond  $0.13 \dot{M}_{\text{Edd}}$  is exactly opposite [50]. This can be seen very clearly for KS 1731-260 where burst observations exist for accretion rates ranging from 0.04 to  $0.4 \dot{M}_{\text{Edd}}$  [50]. Beyond an accretion rate of  $0.13 \dot{M}_{\text{Edd}}$  bursts suddenly become rarer and shorter, indicating that there is not enough hydrogen for the rp-process to reach the first major waiting point at  $A = 64$ . Furthermore, the so-called  $\alpha$  value, the ratio of energy released in between bursts to the energy released in bursts, suddenly increases from 40 (expected if all nuclear burning happens in bursts) to 500-5000. This indicates that beyond  $0.13 \dot{M}_{\text{Edd}}$  most of the nuclear burning occurs outside of bursts in some stable fashion, though current spherically symmetric X-ray burst models predict that all fuel should be burned in bursts. Bildsten 1995 proposed that some nuclear burning proceeds through a slow deflagration front moving across the neutron star surface instead of a rapidly burning burst [46]. Another explanation is given by Narayan and Heyl 2003 [51], who performed a linear stability analysis of the accreted envelope and find a new instability regime of so-called "delayed-mixed bursts" at accretion rates between 0.14 and  $0.25 \dot{M}_{\text{Edd}}$ , where stable burning and X-ray bursts coexist. The predicted accretion rate for the transition into this new regime agrees very well with observations. However, the model also predicts a transition to stable burning and the disappearance of bursts beyond an accretion rate of  $0.25 \dot{M}_{\text{Edd}}$  while there are bursts observed at accretion rates as high as  $0.7 \dot{M}_{\text{Edd}}$  [50]. Furthermore, the "delayed-mixed bursting" behavior (though observed in nature) is not found in recent time-dependent multizone calculations [52] which should in principle give the same result. The lack of understanding of X-ray bursts at accretion rates beyond  $0.13 \dot{M}_{\text{Edd}}$  is particularly bothersome as this is exactly the regime relevant for superbursts (see below).

Another long-standing open question is whether X-ray bursts do in some form contribute to Galactic nucleosynthesis [53,30]. This would be interesting as the rp-process can produce significant amounts of  $^{92,94}\text{Mo}$  and  $^{96,98}\text{Ru}$ . These p-nuclei cannot be produced in sufficient amounts in standard p-process models [54,55]. Costa et al. 2000

[56] proposed that a much larger than theoretically expected  $^{22}\text{Ne}(\alpha, n)$  reaction rate in the s-process, which produces the p-process seeds, could solve the problem. However, theoretical arguments and recent experimental upper limits seem to rule out such a large  $^{22}\text{Ne}(\alpha, n)$  reaction rate [57]. The production of proton-rich Mo and Ru isotopes at another site would also solve the problem of the origin of these isotopes in the solar system. One alternative site that has been proposed is a combination of a weak rp-process with neutron captures in explosions of white dwarfs that reach the Chandrasekhar mass limit by accreting a helium layer [58]. X-ray bursts could in principle be another possibility.

However, the critical question is how matter containing rp-process ashes can be ejected from the surface of a neutron star. The fundamental problem is to overcome the gravitational binding of 200 MeV per nucleon when the nuclear energy release cannot exceed 6 MeV per nucleon. Recently it has been shown that the convective zone developing during the rise of an X-ray burst can extend to sufficiently shallow regions that can be blown off in winds. Such winds are thought to develop during the frequently observed and particularly luminous photospheric expansion bursts [8]. This provides a mechanism to eject ashes from thermonuclear burning into space in a subclass of X-ray bursts. An observational confirmation, for example through detection of spectral features imprinted onto the X-ray flux by the ejected material would be extremely important. However, the material transported to the surface is the ashes of the initial stages of the thermonuclear burning and even for hydrogen rich bursts is dominated by products of the  $\alpha p$  process, mainly  $^{24}\text{Mg}$  and  $^{28}\text{Si}$ , with some smaller amounts of nuclei up to  $A \approx 38$ . Small amounts of  $^{60,62}\text{Zn}$  from processing of the accreted iron are also mixed in. Therefore, this still does not necessarily provide a mechanism to eject heavy rp-process ashes produced during the cooling phase of the X-ray burst when convection has stopped. However, in principle ashes mixed into the burning zone of subsequent bursts or mass ejection through a superburst might be possibilities [8].

Another problem is the total amount of Mo and Ru that can be produced in the Galaxy by X-ray bursts. While Schatz et al. 1998 [30] pointed out that in principle with the ejection of just 1% of the processed matter X-ray bursts could be contributors to Galactic nucleosynthesis, new calculations show [27] that for the rp-process to produce Mo and Ru special circumstances are needed. In the majority of X-ray bursts the rp-process will not produce significant amounts of Mo and Ru. Furthermore, the existence of the later discovered SnSbTe cycle [31] leads to a large co-production of  $^{102}\text{Pd}$  and  $^{106}\text{Cd}$  whenever the rp-process reaches the  $A \approx 90 - 100$  mass region.  $^{102}\text{Pd}$  and  $^{106}\text{Cd}$  do not share the unusual isotopic enhancement found for most proton-rich Mo and Ru isotopes and are produced in sufficient amounts in standard p-process scenarios. It has also been pointed out that the long-lived radioactive p-nucleus  $^{92}\text{Nb}$  might provide important clues as it is co-produced with  $^{92}\text{Mo}$  and other p-nuclei in a photodisintegration type supernova p-process, but is shielded against rp-process contributions by stable  $^{92}\text{Mo}$  [59]. Indeed, traces of extinct  $^{92}\text{Nb}$  present in the early solar system have been detected in primitive meteorites. Estimates using the measured abundance and a galactic chemical evolution model find a  $^{92}\text{Mo}/^{92}\text{Nb}$  production ratio that is very close to the one predicted from supernovae p-process models. However, there are large uncertainties in the galactic chemical evolution modeling and the nuclear physics that determines the  $^{92}\text{Mo}/^{92}\text{Nb}$  ratio in supernovae. In summary it seems to be difficult to explain the origin of proton-rich Mo and Ru isotopes

with the rp-process in X-ray bursts based on current models. Nevertheless, the question of the ejection of burned material in X-ray bursts and its composition should be explored further not only in terms of the nucleosynthesis contribution but also to explore the possibility of future abundance observations through X-ray spectroscopy.

### 2.3. Superbursts and deep carbon burning

Superbursts are rare, extremely powerful X-ray bursts that have been discovered through long term monitoring with the Beppo-SAX Wide Field Camera and the RXTE All-Sky Monitor. They are found in X-ray binary systems that otherwise show regular X-ray bursts. So far, 13 superbursts have been detected from 8 sources, most recently in GX 17+2 [60] (see [61] for a recent observational overview). Compared to the regular bursts, superbursts are a factor of 1000 times more energetic, they last many hours as opposed to 10-100s, and their recurrence time is around a year instead of hours to days. Superbursts show the same spectral behavior than normal X-ray bursts, and in one case it was possible to detect ms oscillations with RXTE that show a behavior similar to the oscillations in normal bursts [62]. Superbursts are therefore likely to be of thermonuclear origin.

Superbursts most likely occur when carbon in the ashes from regular bursts ignites deep in the neutron star's liquid surface ocean [11,64,63]. Cumming and Bildsten 2001 [64] pointed out that the presence of heavy nuclei beyond iron in the ashes plays an important role as they increase the opacity of the layer and therefore affect the ignition depth. Schatz et al. 2003 [65] investigated in more detail the actual nuclear processes occurring during a superburst and found that in addition to carbon fusion, photodisintegration of heavy elements plays an important role. Once carbon burning heats the layer to 1-2 GK (depending on the detailed composition) the extremely temperature sensitive photodisintegration reactions on heavy nuclei trigger a photodisintegration runaway that leads to a rapid rise of the temperature up to 7 GK. This drives the composition into Nuclear Statistical Equilibrium (NSE), which at superburst conditions contains mainly nuclei around  $^{66}\text{Ni}$ . Depending on the initial composition set by the ashes of the regular bursts the photodisintegration of heavy elements into Ni can contribute up to about 50% of the total superburst energy.

For ashes typical of explosive hydrogen burning carbon ignition occurs around a density of  $10^9 \text{ g/cm}^3$  - about 3 orders of magnitude larger than for ordinary X-ray bursts. The much higher ignition depth explains the longer recurrence time and the higher total energy as more matter needs to be accumulated to trigger the burst. The longer burst duration matches the radiative cooling timescale from the ignition layer. The carbon ignition model also explains the observed interaction of superbursts with normal bursts. The increasing heat flux at the surface shortly after superburst ignition triggers the explosive burning of the hydrogen and helium in the upper layers leading to the observed "precursors" - a regular X-ray bursts preceding the superburst [66]. The long cooling timescales lead to an increased surface heat flux for many weeks explaining the suppression of regular bursts after a superburst.

Superbursts are an important probe for the properties of neutron stars. As they occur deeper than regular X-ray bursts, they are more sensitive to the thermal properties of the crust and core cooling models. As Brown [67] showed recently, the mere existence of superbursts can put tight constraints on the thermal conductivity of the neutron star



crust and on the rate of neutrino cooling in the core.

The main open question concerning superbursts is the origin of a sufficient amount of carbon (at least a few % mass fraction) in the ashes of hydrogen and helium burning on the surface. Recent one-zone models of X-ray bursts showed that when one includes the full rp-process hydrogen is consumed completely leading to a brief helium burning phase at the end of the burst that produces some carbon. However, more recent calculations [27] that follow a series of bursts, demonstrated that any carbon leftover in the ashes of a specific burst is destroyed via the capture of residual helium triggered by the heat from the next burst. A key issue in this problem is the unexplained regular burst behavior at accretion rates beyond  $0.13 \dot{M}_{\text{Edd}}$ , which is just the range relevant for superbursts (see Sec. 2.2). As discussed above, at these accretion rates some fuel is likely burned steadily and not in bursts. Such stable burning could in principle produce the amount of carbon needed to explain the superburst phenomenon [36].

Except for the carbon fusion rate that triggers the unstable burning uncertainties in the nuclear physics of the processes during superbursts are not likely to be important. The matter is quickly driven into NSE, where final composition and energy generation are determined by ground state masses and partition functions of experimentally well studied nuclei near stability. However, the nuclear physics uncertainties in regular X-ray bursts, in particular in the rp-process, together with the astrophysical puzzles associated with them prevent a reliable calculation of the X-ray burst ashes which serve as the fuel for superbursts. This is a major obstacle towards a full understanding of superbursts and a solution of this problem is critical for using superbursts as reliable probes for the properties of accreting neutron stars.

## 2.4. Crust processes

The neutron star crust serves as an interface between the physics of the neutron star and observations. One direct observable is the quiescent luminosity from the crust of neutron stars in transient X-ray binary systems (so-called Soft X-ray Transients). These systems are characterized by a thermal accretion disc instability that turns the accretion onto the neutron star on and off with periods ranging from months to decades [68,69]. It has been argued [72,73] that the quiescent luminosity that is observed from Soft X-ray Transients after the accretion has turned off, is the thermal radiation from the cooling neutron star crust. This offers a pathway to distinguish neutron star systems from black hole systems, and to determine neutron star radii provided the observed spectrum can be accurately modeled [74] and the distance to the source is known.

In addition, luminosity measurements directly constrain the thermal state of the crust, which in turn can be used as a probe for neutron star physics such as the existence of enhanced neutrino cooling processes, superfluidity, or exotic phases of nuclear matter [70, 71]. Wijnands 2004 [76] gives an extensive review of the observational status concerning the detection of soft X-ray transients in quiescence. The majority of X-ray transients have periods of the order of months and crust luminosity measurements can be used to determine the limit cycle thermal state of the crust [72]. In long period transients (so-called quasi-persistent sources), which turn off for years to decades repeated observations during the off state offer the unique opportunity to measure the crust cooling behavior of an accreting neutron star as a function of time [75]. This has recently become possible

in two cases - for KS 1731-260, which turned off early in 2001 a drop of the surface luminosity was followed in 4 measurements over 2.5 years [76]. Similarly, for MXB 1659-29 3 measurements over several years were performed [77]. In both cases the decrease in luminosity of about a factor of 8 over a few years is consistent with the observed decrease in effective temperature further supporting the assumption that one observes a cooling neutron star crust. Interestingly, comparison with crust models shows that such a rapid drop in luminosity can only be reproduced when assuming enhanced neutrino cooling in the neutron star core. However, the detection of a superburst from KS 1731-260 during its on-state points to a hot crust and seems to rule out enhanced neutrino cooling [67]. At this point a solution to this puzzle is not in sight, but clearly a better understanding of the nuclear physics underlying both probes - superbursts and the neutron star surface luminosity behavior - would be important.

The neutron star crust composition and its thermal state also affect the crust electrical conductivity. This is important for another fundamental open question - the existence of two classes of X-ray binaries: X-ray pulsars characterized by high magnetic fields that funnel the accretion flow onto the polar caps, and X-ray bursters with low magnetic fields. While a long term decay of magnetic fields seems to be a likely explanation, neither the origin of the magnetic fields nor the mechanism of the field decay are understood [78,79,80].

As pointed out above, the initial composition of the neutron star crust is determined by the ashes of the surface burning processes such as X-ray bursts and superbursts. The ongoing accretion compresses the ashes continuously and converts it into deeper and deeper layers of the crust. The rising electron Fermi energy initiates a sequence of electron captures, which beyond neutron drip are accompanied by neutron emission. In the inner crust of the neutron star the nuclei have finally low enough charge numbers to enable pycnonuclear fusion reactions [81,82,83]. All these reactions generate heat and might also deform the crust leading to the possibility of gravitational wave emission if the neutron star is spinning rapidly [84,85].

Together with the rp-process and the nuclear reactions during superbursts these crust processes determine the crustal heating and the crust composition, which in turn strongly affects thermal and electrical crust conductivities. Therefore, the nuclear physics of a wide range of processes needs to be understood before observations can be translated into quantitative constraints of neutron star properties. These processes include all nuclei from the proton drip line to the neutron drip line up to a maximum mass number that is set by the endpoint of the rp-process, with a maximum at  $A \approx 106$  set by the Sn-Sb-Te cycle.

So far, the nuclear processes in the crust of an accreting neutron star have only been explored in a schematic way assuming single nuclide compositions, zero temperature and infinitely fast electron capture at threshold. While these are not unreasonable assumptions for a first exploration of nuclear crust processes, more detailed simulations would be needed to determine the impact of nuclear physics uncertainties such as electron capture thresholds, the location of the neutron drip line, electron capture rates, and pycnonuclear fusion rates on crust studies and observables. In addition, crust processes strongly depend on the initial composition set by the ashes of X-ray bursts and superbursts. The nuclear physics uncertainties in the rp-process therefore strongly affect the physics of the crust. Already, the inclusion of reactions beyond Ni in the rp-process has had a significant

impact in demonstrating that the crust consists most likely not of a pure single nuclide lattice, for example Fe, but of a wider range of nuclear species. This is a consequence of the long waiting points in the rp-process beyond  $^{56}\text{Ni}$  that lead to a spreading in the final abundance distribution. First estimates show that such an impure crust has a much reduced thermal and electrical conductivity [79,86].

### 3. Nuclear physics needs

The surface of accreting neutron stars is characterized by a wide range of nuclear processes ranging from fragmentation at infall, over thermonuclear burning in X-ray bursts and superbursts, to electron captures and pycnonuclear fusion reactions in the neutron star crust. These processes involve the majority of the nuclei between the proton and the neutron drip line up to a maximum mass number set by the endpoint of the rp-process. In this picture, the rp-process during X-ray bursts (and maybe during stable hydrogen burning as well) plays a central role as it directly determines one of the key observables, the observed X-ray bursts, and because it sets the initial composition for all the deeper processes. At the same time, the nuclear physics and its impact on observables has been explored for the rp-process to a much greater extent than for any of the other processes on accreting neutron stars. We therefore concentrate in the following on the open nuclear physics questions related to the rp-process. Earlier reviews of the experimental and theoretical nuclear physics aspects of the rp-process can be found in [87,29,30,88,32].

As shown in Fig. 1 [30] the rp process in X-ray bursts follows a path away from the valley of stability through  $\beta$ -unstable nuclei. It is dominated by  $(p,\gamma)$  reactions and  $\beta$ -decays and extends up to the mass  $\sim 64$ -106 region depending on the astrophysical conditions. For lighter nuclei (up to mass  $\sim 40$ ) the  $(\alpha,p)$  reaction can compete successfully with proton capture at X-ray burst temperatures. The  $(\alpha,p)$  reaction followed by a radiative proton capture  $(p,\gamma)$  is a very effective way for the production of heavier nuclei without waiting for an intermediate beta decay. This so-called  $\alpha p$  process is thought to determine the early phase of an X-ray burst lightcurve when the increasing temperature enables  $(\alpha,p)$  reactions at successively heavier nuclei. Depending on the peak temperature reached in a particular burst the final  $\alpha p$ -process can extend up to Sc, mainly through the sequence  $^{14}\text{O}(\alpha,p)^{17}\text{F}(p,\gamma)^{18}\text{Ne}(\alpha,p)^{21}\text{Na}(p,\gamma)^{22}\text{Mg}(\alpha,p)^{25}\text{Al}(p,\gamma)^{26}\text{Si}(\alpha,p)^{29}\text{P}(p,\gamma)^{30}\text{S}(\alpha,p)^{33}\text{Cl}(p,\gamma)^{34}\text{Ar}(\alpha,p)^{37}\text{K}(p,\gamma)^{38}\text{Ca}(\alpha,p)^{21}\text{Sc}$ . At several points along the path short-lived  $\beta$ -decays can compete leading to several parallel flows.

Most of the nuclei probed in the rp-process do not exist as stable nuclei but the majority of them have been produced in the laboratory, as indicated in Fig. 1. Besides particle stability half-lives and masses are the other crucial input parameters for determining the reaction paths in the rp-process.

#### 3.1. Nuclear Masses

In the rp process proton capture is favored compared to  $\beta$ -decay until a nucleus with a small  $(p,\gamma)$  Q value is reached where an equilibrium between  $(p,\gamma)$  capture and its inverse  $(\gamma,p)$  photodisintegration is established. At this point the rp process has to wait until via  $\beta^+$  decay a less proton-rich nucleus is formed. Since the equilibrium depends exponentially on the  $(p,\gamma)$  Q-value the mass of the waiting point nucleus itself as well the masses of the isotones which can be reached via one and two proton capture reactions

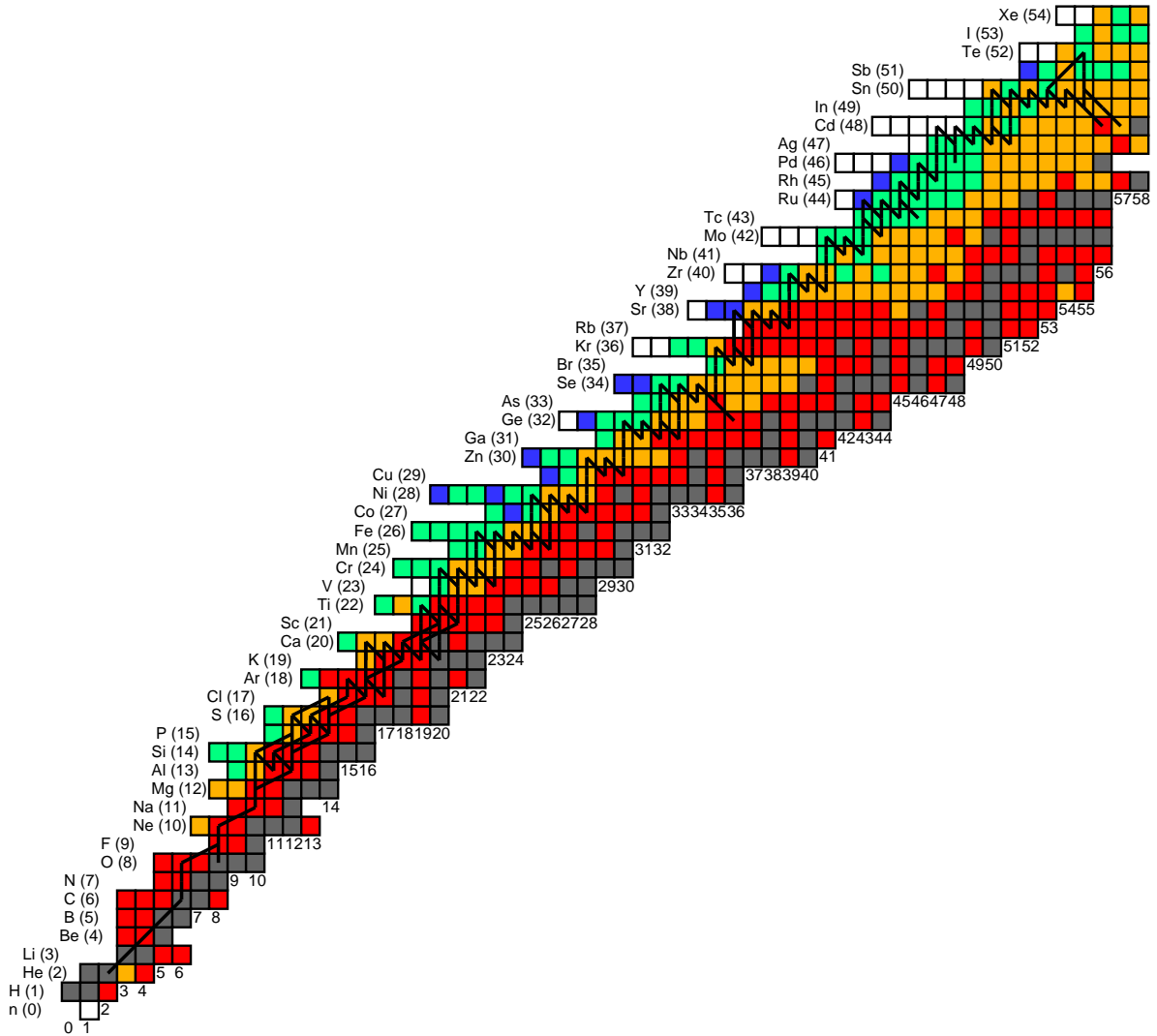


Figure 1. The main path of the rp-process in a one-zone X-ray burst model [31]. Stable nuclides are grey, nuclides with masses experimentally known to better than 10 keV are red, other nuclides with experimentally known masses are orange, nuclides with experimentally known half-lives but unknown masses are green, and nuclei that have only been identified in experiments are blue.

have to be known with a precision of about  $kT \approx 100$  keV (with  $k$  being the Boltzmann constant and  $T$  a typical temperature).

Nuclear masses are also important for the determination of proton capture rates. For many of these rates along the rp-process path Q-values are too high to establish a (p, $\gamma$ )-( $\gamma$ ,p) equilibrium at all times, but they are still low enough for a few individual resonances to dominate the reaction rate. Because of the exponential dependence of the proton capture rate on the resonance energy, masses (and excitation energies) need to be known to better than 10 keV in those cases. As Fig. 1 shows, for most of the rp-process, especially beyond Ti, masses are still not accurate enough for reliable reaction rate calculations or the planning of direct reaction rate measurements with radioactive beams.

For the most part masses in the rp-process can be theoretically predicted using extrapolations [97] or, beyond the  $N = Z$  line, Coulomb shift calculations [98]. In some cases where the mass or the mirror nucleus is known with high accuracy, the latter method can reach 100 keV accuracy. While this represents a considerable improvement over global mass models [30], the uncertainties in theoretical mass predictions are still too large for astrophysical applications. Experimental data are therefore needed.

Considerable progress has been made during the past years at various laboratories to measure masses of rp process nuclei (see Fig. 1), but much remains to be done [99]. As Fig. 1 shows, already beyond magnesium not all reaction Q-values are known to better than 10 keV, and beyond vanadium hardly any are sufficiently accurate. One new technique are mass measurements of unstable nuclei in the ESR storage ring at GSI using an isochronous tune and a time-of-flight detector [89,90]. The advantage of this technique is the low half-life limit of a few microseconds that includes all particle bound nuclei. Conventional  $\beta$ -endpoint [91] and time-of-flight techniques [92] have also been used. A major step forward in this field, however, was the use of Penning traps with radioactive proton rich beams. These systems can achieve the needed accuracies of 10-100 keV or better for even the heaviest rp-process nuclei. Several of these mass spectrometers are now operational worldwide [93,94,95,96]. The nuclei are produced using various nuclear reactions, they are thermalized, cooled and then injected into the Penning trap. For a mass measurement the isotope has to live at least 100 ms, a condition which is fulfilled for practically all rp-process nuclei.

Along the proton dripline the pairing force can lead to the stability of certain even- $Z$  nuclei while the neighboring  $Z+1$  nuclei are proton unstable. Examples are the  $N=34$  and  $36$   $N=Z$  nuclei  $^{68}\text{Se}$  and  $^{72}\text{Kr}$  which have relatively long half-lives of 35.5 s and 17 s, respectively, while the isotones  $^{69}\text{Br}$  and  $^{73}\text{Rb}$  are particle-unbound. For the  $^{68}\text{Se}$  case the  $\beta$ -decay waiting point can be bridged through the successive capture of two protons via the particle-unstable  $^{69}\text{Br}$  leading to the particle-stable nucleus  $^{70}\text{Kr}$ . The mass of the particle-unstable  $^{69}\text{Br}$  can only be measured through transfer reactions using radioactive beams. However, an estimate for the masses of these unstable nuclei can be obtained using Coulomb displacement energies from mirror nuclei [98].

A recent mass measurement of  $^{68}\text{Se}$  [100] together with estimates of the mass of  $^{69}\text{Br}$  has led to the conclusion that  $^{68}\text{Se}$  remains a waiting point in the rp process. Similar results have been obtained for  $^{64}\text{Ge}$  [101] and  $^{72}\text{Kr}$  [102]. In the latter case the masses of  $^{72-74}\text{Kr}$  had been measured providing together with Coulomb shift calculations good estimates

for the masses of the entire relevant isotone chain  $^{72}\text{Kr}$ ,  $^{73}\text{Rb}$ , and  $^{74}\text{Kr}$ . As in the case of  $^{68}\text{Se}$  it was found that  $^{72}\text{Kr}$  probably remains a significant waiting point in the rp-process, but it was also pointed out that because of uncertainties in the proton capture rates final conclusions cannot be drawn yet.

In summary, for most of the important waiting point nuclei such as  $^{64}\text{Ge}$ ,  $^{68}\text{Se}$ ,  $^{72}\text{Kr}$  and  $^{104}\text{Sn}$ , masses and half lives are now known with sufficient accuracy. However, what is needed for rp-process calculations are proton capture Q-values. For  $^{64}\text{Ge}$ ,  $^{68}\text{Se}$ , and  $^{72}\text{Kr}$  the mass of the proton capture isotone is not yet known experimentally. For  $^{104}\text{Sn}$  the proton capture Q-value has been determined from the detection of proton decay in  $^{105}\text{Sb}$  [103,104]. However, the two experiments give somewhat conflicting results of either  $478\pm 15$  keV or  $550\pm 30$  keV for the proton energy. Therefore, despite the considerable progress that has been made, accurate experimental proton capture Q-values are still not available for the major rp-process waiting points.

### 3.2. $\beta$ -decay half-lives

$\beta$ -decay half-lives are critical for rp-process calculations as they determine the timescale for the buildup of heavier elements and energy generation as well as the final abundance distribution. As Fig. 1 shows, most of the important  $\beta$ -decay half-lives in the rp-process have been measured in radioactive beam experiments with a few exceptions such as  $^{95,96}\text{Cd}$ . In principle, theoretical corrections need to be applied to the experimental half-lives to account for the actual astrophysical environment during an X-ray burst. This has been investigated by Fuller, Fowler and Newman 1982 [105] and more recently by Pruet et al. 2003 [106], who tabulate corrected weak decay rates as a function of temperature and density for use in X-ray burst calculations. At temperatures of up to 2 GK low-lying states can be thermally populated, and the decay rates from these states can differ from the ground state decay rates measured in experiments. As the most important waiting point nuclei in the rp-process tend to be even-even nuclei with relatively high-lying first excited states this is usually not a large effect [30]. Exceptions might occur around  $^{80}\text{Zr}$  where a large ground state deformation lowers the energy of the first excited state considerably. The second correction is needed to take electron capture into account properly. Nuclei in the X-ray burst environment are fully ionized and bound state electron capture that might be present in the laboratory, is not important in the stellar environment. On the other hand, electron densities during X-ray bursts can be sufficiently large for continuum electron capture to play a role. However, as the majority of the important rp-process waiting points are far from stability and have large  $\beta$ -decay Q-values electron capture in the laboratory and in the star is in most cases negligible at the 10% level. In that case the use of measured terrestrial half-lives in rp-process calculations is appropriate. However, such corrections can become important closer to stability, for example at the onset of the rp-process below Zn and in particular X-ray bursts where the rp-process ends in the  $A = 60 - 72$  mass range and moves closer to stability during the final cooling phase.

$\beta$ -decays in the rp-process are not only important bottle-necks in the reaction flow, but serve also as the major nuclear energy source owing to their large positive Q-values. To accurately determine the energy production of the rp-process, the actual  $\beta$ -decay scheme

needs to be known to determine the amount of energy that is lost via neutrino emission. While most of the  $\beta$ -decay half-lives are measured, in many cases the actual  $\beta$ -strength functions have not been determined experimentally. Therefore theoretical  $\beta$ -decay calculations [105,106] have to be used to determine the neutrino energy loss during X-ray bursts.

### 3.3. Astrophysical Reaction Rates.

Because the majority of nuclei involved in the rp process are unstable most of the reaction rates so far had to be estimated based on theoretical grounds. While a statistical Hauser-Feshbach treatment is possible for nuclei with high  $(p,\gamma)$  Q-values where states at high excitation energy are being populated [107], in many cases the individual level structure of a particular nucleus can dominate the reaction rate. Shell model calculations have been performed for these cases in the sd- [108] and fp-shell [109] and these rates are used widely in rp-process calculations. However, the accuracy of the predicted excitation energies of individual levels is at most around 100 keV. For resonant reaction rates this translates into uncertainties of many orders of magnitude. Even in cases where the level energies have been determined experimentally, an uncertainty of at least a factor of 2-3 remains. For this reason direct measurements of critical reactions along the rp-process path are urgently needed.

Reaction rates in the rp-process need to be determined for a wide range of temperatures up to about 2 GK. While X-ray bursts ignite at temperatures around 0.2 GK, the lower temperature limit for the reaction rate determination is usually set by the condition that the reaction rate timescale has to be less than the typical X-ray burst timescale of  $\sim 10$  s. For typical X-ray burst conditions with hydrogen mass fractions of 0.5 and mass densities of  $10^6$  g/cm<sup>3</sup> one finds that a proton induced reaction rate is important once it exceeds  $2 \times 10^{-7}$  cm<sup>3</sup>/s/mole. As an example, proton capture rates on Ne, Cl, and Ge need to be known for temperatures above 0.2, 0.3, and 0.5 GK respectively.

With the exception of a few long-lived nuclei (e.g. <sup>18</sup>F, <sup>22</sup>Na, <sup>26</sup>Al, <sup>44</sup>Ti and <sup>56</sup>Ni) which could be produced as targets in standard kinematics experiments using proton or alpha beams all other isotopes along the rp path have very short half-lives and require the use of the so-called inverse kinematics, where a proton or He target is bombarded with a heavier radioactive beam. Some of these beams have become available during the last 15 years at several laboratories, leading to a new era in nuclear astrophysics. Since the beam intensities at these first generation facilities are still 3-5 orders of magnitude below the intensities available with stable beams new, high efficiency detector systems optimized for reaction studies in inverse kinematics had to be developed. So far only a handful of experimental  $(p,\alpha)$  and  $(\alpha,p)$  reaction rates have been measured directly during the past few years. The direct measurement of a  $(p,\gamma)$  reaction with a radioactive beam has only succeeded in two cases, the <sup>13</sup>N $(p,\gamma)$ <sup>14</sup>O reaction at Louvain-la-Neuve [111,112] and the <sup>21</sup>Na $(p,\gamma)$ <sup>22</sup>Mg reaction at TRIUMF [113]. The rates of these reactions are discussed below.

For the many cases where a direct measurement of the reaction rate is still outside the experimental capabilities, indirect approaches can be used. They are important when resonances are too weak, when the exact location of the resonances are not known or

when the radioactive beams needed for a direct measurement can not yet be produced. They are also needed to determine capture rates on low-lying thermally excited states in the target, which at the extreme temperatures reached in X-ray bursts can be important in some cases. For example, elastic scattering can be used to locate resonances or determine their total widths, and transfer reactions can give information about partial widths and decay properties. Gamma detector arrays, such as GAMMASPHERE [114] or SEGA [115] with their excellent energy resolution can also be used to identify states that dominate the reaction rate for nuclei away from stability.

In some cases it is more convenient to measure the time-inverse of the reaction that actually occurs in the astrophysical environment. The information on the forward reaction is then obtained through the principle of detailed balance. Coulomb dissociation is the time-inverse of a direct capture reaction and has been successfully used in some (mainly lighter) systems, e.g.  $^{13}\text{N}(\text{p},\gamma)^{14}\text{O}$  [116,117]. The technique can give an increase in yield by a factor of  $10^5$  over the forward capture reaction and can thus be used with relatively weak radioactive beams. It probes, however, only the  $\gamma$ -transition to the ground state and there are additional difficulties with transitions of mixed multipolarity.

Other examples of the successful use of time-inverse reactions which are of importance to the study of X-ray bursts are studies of  $(\alpha,\text{p})$  reactions through their time-inverse partner  $(\text{p},\alpha)$ , thereby avoiding the use of a He target. A drawback of this technique is that contributions from excited states in the final nucleus have to be determined separately, e.g. through a measurement of elastic and inelastic scattering.

In the following the results from recent measurements of reaction rates in X-ray bursts with radioactive beams or targets using both, direct and indirect techniques are briefly discussed.

### 3.3.1. The triple- $\alpha$ reaction

The rate for the triple- $\alpha$  reaction which triggers the X-ray bursts and serves as the starting point and major initial bottle-neck of the rp-process (see Fig.1) has recently seen some changes resulting from the spin and energy determination of a resonance at  $E_x \sim 11$  MeV [110]. The main modifications are an increase in the rate at low temperatures (below  $5 \times 10^7$  K) and a steep decrease by more than an order of magnitude at temperatures above  $2.5 \times 10^9$  K. More calculations need to be done to investigate the effect of the changes in the reaction rate on the rp process.

### 3.3.2. The $^{13}\text{N}(\text{p},\gamma)^{14}\text{O}$ Reaction

The  $^{13}\text{N}(\text{p},\gamma)^{14}\text{O}$  reaction can bypass the slow  $\beta$ -decay of  $^{13}\text{N}$  ( $T_{1/2}=9.96\text{m}$ ) leading to the so-called hot CNO cycle where the energy production is independent of the temperature and limited by the beta decays of  $^{14}\text{O}$  ( $T_{1/2}=70.6$  s) and  $^{15}\text{O}$  ( $T_{1/2}=2.03$  m). This reaction was measured directly in a pioneering experiment with a  $^{13}\text{N}$  beam at Louvain-la-Neuve [111,112] as well as with indirect (Coulomb dissociation) techniques at RIKEN [116] and GANIL [117]. The results from these experiments agree among each other giving a width  $\Gamma_\gamma$  of  $3.0 \pm 0.5$  eV and a resonance strength of  $9 \pm 1.5$  eV. A recent measurement extracting the Asymptotic Normalization Coefficient (ANC) from a transfer



reaction measurement has led to a slight modification of the reaction rate which agrees with the tabulated values [118] at temperatures above  $T_9 \sim 0.5$  but exhibits an increase by a factor of 1.5-2 below  $T_9 \sim 0.25$ [119].

### 3.3.3. The $^{14}\text{O}(\alpha, \text{p})^{17}\text{F}$ Reaction.

This reaction has been studied through its time inverse  $^{17}\text{F}(\text{p}, \alpha)^{14}\text{O}$  reaction at ANL[120] and ORNL[121]. The transitions to the first excited  $1/2^+$  state in  $^{17}\text{F}$  was addressed through independent measurements of the  $^{17}\text{F}(\text{p}, \text{p}')^{17}\text{F}$  reaction[122,123]. The cross sections in these two experiments were found to agree within their experimental uncertainties. In a more recent experiment this reaction was measured directly with a  $^{14}\text{O}$  beam and a cryogenic He target[124]. There is some disagreement between the direct and indirect measurements that need to be addressed in future measurements.

### 3.3.4. The $^{17}\text{F}(\text{p}, \gamma)^{18}\text{Ne}$ Reaction.

This reaction rate is part of the  $(\alpha, \text{p})$  process following the  $^{14}\text{O}(\alpha, \text{p})^{17}\text{F}$  reaction. It depends critically on the exact location of a  $3^+$  state which is expected from mirror symmetry arguments at an energy of 4.5 MeV. This state was first unambiguously identified in experiments with  $^{17}\text{F}$  beams at ORNL[125,126,127]. From the resonant strength whose value still depends somewhat on properties of the mirror nucleus one finds that the reaction rate for temperatures above  $T_9 \sim 0.5$  is determined by this state.

### 3.3.5. The $^{18}\text{Ne}(\alpha, \text{p})^{21}\text{Na}$ reaction.

This reaction was studied directly with a  $^{18}\text{Ne}$  beam and an active He target[128,129] at excitation energies which, however, are too high to be relevant for X-ray bursts. Furthermore, the cross sections obtained in these experiments seem to exhaust the Wigner limits for states at an excitation energy of 11 MeV. Recent experiments using the indirect time-inverse  $^{21}\text{Na}(\text{p}, \alpha)^{18}\text{Ne}$  approach have found considerably smaller yields[130]. These discrepancies require further studies and experiments at several radioactive beam facilities are planned for the future.

### 3.3.6. The $^{19}\text{Ne}(\text{p}, \gamma)^{20}\text{Na}$ Reaction.

As part of the  $^{15}\text{O}(\alpha, \gamma)^{19}\text{Ne}(\text{p}, \gamma)^{20}\text{Na}$  chain this reaction is at the onset of the rp process. A direct study using a  $^{19}\text{Ne}$  beam and detecting the delayed decay products from  $^{20}\text{Na}$  [131,132] has so far only given an upper limit of the first state above the proton threshold (see also [133]). However, even the spin of this state is still being debated[134,135,136,137] and, thus, the value of the reaction rate for this reaction is still uncertain by orders of magnitude.

### 3.3.7. The $^{21}\text{Na}(\text{p}, \gamma)^{22}\text{Mg}$ Reaction.

This reaction is again part of the  $(\alpha, \text{p})$  process, following the  $^{18}\text{Ne}(\alpha, \text{p})^{21}\text{Na}$  reaction. The resonant strengths of seven resonances in  $^{22}\text{Mg}$  have been directly measured with a  $^{21}\text{Na}$  beam at TRIUMF[138,139].

### 3.3.8. The $^{22}\text{Na}(p,\gamma)^{23}\text{Mg}$ Reaction.

This reaction has been studied by direct and indirect techniques. Bombarding a radioactive  $^{22}\text{Na}$  ( $T_{1/2}=2.6$  y) target with a proton beam in two experiments has led to a reaction rate which is smaller by about an order of magnitude when compared to a pure theoretical estimate[140,141]. More recent indirect measurements using GAMMAS-PHERE resulted in an increase of this rate due to the addition of new resonances which were not included in the previous analyses[142].

### 3.3.9. The $^{22}\text{Mg}(p,\gamma)^{23}\text{Al}$ Reaction

$^{22}\text{Mg}$  is a potential local waiting point where proton capture competes with the  $(\alpha,p)$  reaction. A recent measurement of the  $^{24}\text{Mg}(^7\text{Li},^8\text{He})^{23}\text{Al}$  reaction established the mass and the energy of the first excited state in  $^{23}\text{Al}$ [143]. The astrophysical reaction rate for the  $^{22}\text{Mg}(p,\gamma)$  reaction was then obtained using a spectroscopic factor based on shell model calculations. A recent measurement of Coulomb dissociation of  $^{23}\text{Al}$ [144] resulted in a resonance strength which is in good agreement with the value used in Ref.[143]. These measurements have reduced the uncertainties of the  $(p,\gamma)$  rate considerably. However, because of its small Q-value the  $^{22}\text{Mg}(p,\gamma)^{23}\text{Al}$  reaction is in equilibrium with its inverse reaction  $^{23}\text{Al}(\gamma,p)^{22}\text{Mg}$  and, thus, very little  $^{23}\text{Al}$  is produced. The influence of the 2-proton capture reaction on  $^{22}\text{Mg}$  forming  $^{24}\text{Si}$  which becomes important at higher temperatures has been discussed in Ref.[145].

### 3.3.10. The $^{32}\text{Cl}(p,\gamma)^{33}\text{Ar}$ Reaction.

The reaction rate used in previous calculations was entirely based on shell-model calculations with uncertainties in the excitation energy around 100 keV. Populating the states in  $^{33}\text{Ar}$  above the proton threshold via the  $^{34}\text{Ar}(p,d)^{33}\text{Ar}$  reaction and studying their  $\gamma$  decay has allowed to put much smaller error bars on the excitation energies of some of the critical levels[146]. This has reduced the uncertainty in the reaction rate from 3 orders of magnitude to a factor of 3 at the critical temperatures around 0.3 GK and to a factor of 6 at the highest X-ray burst temperatures. For high temperatures additional states, which have not been identified so far might contribute as well. Further studies for this system are clearly desirable.

### 3.3.11. The $^{56}\text{Ni}(p,\gamma)^{57}\text{Cu}$ Reaction.

The sequence of  $(\alpha,p)$  and  $(p,\gamma)$  reactions leading to the formation of heavier nuclei in a X-ray bursts proceeds mainly through the nucleus  $^{56}\text{Ni}$  which is a waiting point in the reaction flow. Because of the closed-shell nature of  $^{56}\text{Ni}$  the Q value for the  $^{56}\text{Ni}(p,\gamma)^{57}\text{Cu}$  reaction is quite small ( $Q=0.695$  MeV) so that the cross section can not be reliably estimated using statistical model calculations. The rate is dominated by transitions to the first two excited states in  $^{57}\text{Cu}$ . A direct measurement of the cross section is impossible using present-day capabilities and thus indirect methods have to be employed. In such an approach the one-particle transfer reactions  $^{56}\text{Ni}(d,p)^{57}\text{Ni}$ [147,148] and  $^{56}\text{Ni}(^3\text{He},d)^{57}\text{Cu}$ [149] have been measured with a weak ( $3\times 10^4/s$ )  $^{56}\text{Ni}$  beam. Using the spectroscopic factors from these measurements, calculated proton penetrabilities, and  $\gamma$ -widths from the  $^{57}\text{Ni}$  mirror [150] an estimate for the  $^{56}\text{Ni}(p,\gamma)^{57}\text{Cu}$  reaction rate could be determined which

was found to be 10 times larger than previous estimates[29,150]. For temperatures above 1 GK the reaction rate was later slightly revised due to an improved treatment of the  $\gamma$ -widths [151].

In addition to radioactive beam measurements, experiments with stable beams continue to play an important role for the lower part of the  $\alpha$ p- and rp-process reaction chains below about Ca. Recent examples of experiments that use transfer reactions with stable beams to reach nuclei in the rp-process include measurements using the  $^{20}\text{Ne}(^3\text{He},\alpha)^{19}\text{Ne}$  reaction at ANL[152], the  $^{21}\text{Ne}(p,t)^{19}\text{Ne}$  reaction at KVI [153,154], the  $^{24}\text{Mg}(^4\text{He},^6\text{He})^{22}\text{Mg}$  reaction at RCNP [155], the  $^{25}\text{Mg}(^3\text{He},^6\text{He})^{22}\text{Mg}$  reaction at Yale [156], the  $^{24}\text{Mg}(p,t)^{22}\text{Mg}$  reaction at CNS Tokyo[157], the  $^{12}\text{C}(^{12}\text{C},2n)^{22}\text{Mg}$  reaction at ANL[158], the  $^{24}\text{Mg}(^7\text{Li},^8\text{He})^{23}\text{Al}$  and  $^{28}\text{Si}(^7\text{Li},^8\text{He})^{27}\text{P}$ [143] reactions at MSU and a variety of reactions to access states in  $^{19}\text{Ne}$ ,  $^{26}\text{Si}$  and  $^{26}\text{Al}$  at ANL, Notre Dame, Princeton, and Yale.

From the compilation of the experimental reaction rates given above it can be seen that only a small percentage of the astrophysical reaction rates which are relevant for X-ray bursts are based on experimental data. For most of them only theoretical estimates are available. The same holds for many electron capture rates and pycnonuclear fusion cross sections involving neutron-rich nuclei. While significant progress is expected with existing facilities, a new generation of radioactive beam facilities such as RIA is needed to address all the nuclear physics questions related to accreting neutron stars in X-ray binaries.

The authors thank Ed Brown for useful discussions concerning this manuscript. This work has been supported by the Joint Institute for Nuclear Astrophysics (JINA) under NSF grant PHY 02-16783. H.S. acknowledges support from NSF grant PHY 0110253. K.E.R is supported by the U.S. Department of Energy, Office of Nuclear Physics under contract W-31-109-ENG-38.

## REFERENCES

1. D. Psaltis, astro-ph/0410536 (2004).
2. T.E. Strohmayer and L. Bildsten, Compact Stellar X-ray Sources, ed. W. H. G. Lewin and M. van der Klies (Cambridge: Cambridge Univ. Press), astro-ph/0301544 (2003).
3. L. Bildsten, P. Chang, and F. Paerels, Ap. J. 591 (2003), L29.
4. J. Cottam, F. Paerels, and M. Mendez, Nature 420 (2002) 51.
5. L. Bildsten, E. E. Salpeter, and I. Wasserman Ap. J. 384 (1992) 143.
6. T. E. Strohmayer, and A. R. Villarreal Ap. J. 614 (2004) 121.
7. P. C. Joss, Nature 270 (1977) 310.
8. N. N. Weinberg, L. Bildsten, and H. Schatz, Ap. J. 639 (2006) 1018.
9. J. Grindlay et al. Ap. J. 205 (1976) L127.
10. R. D. Belian, J. P. Conner, and W. D. Evans, Ap. J. 206 (1976) L135.
11. S. E. Woosley and R. E. Taam, Nature 263 101 (1976).
12. L. Maraschi and A. Cavaliere, Highlights of Astronomy 4 (1977) 127.
13. D. Q. Lamb and F. K. Lamb, Ap. J., 220 (1978) 220.
14. C. J. Hansen and H. M. Van Horn, Ap. J. 195 (1975) 735.
15. L. Bildsten, in *The Many Faces of Neutron Stars*, edited by A. Alpar, L. Bucceri, and

- J. Van Paradijs (Dordrecht, Kluwer, 1998), pp. astro-ph/9709094.
16. W. H. G. Lewin, J. van Paradijs, and R. E. Taam, *Space Sci. Rev.* 62 (1993) 233.
  17. T. E. Strohmayer et al. *Ap. J.* 469 (1996) L9.
  18. A. Cumming et al. *Ap. J.* 564 (2002) 343.
  19. A. L. Piro and L. Bildsten, submitted to *Ap. J.* (2005), astro-ph/0502546.
  20. A. Cumming and L. Bildsten, *Ap. J.* 506 (1998) 842.
  21. P. N. McDermott, H. M. van Horn, and C. J. Hansen, *Ap. J.* 325 (1988) 725.
  22. D. Chakrabarty et al. *Nature* 424 (2003) 42.
  23. T. E. Strohmayer et al. *Ap. J.* 596 (2003) L67.
  24. M. P. Munro, D. K. Galloway, and D. Chakrabarty, *Ap. J.* 608, (2004), 930.
  25. T. E. Strohmayer, astro-ph/0401465 (2004).
  26. S. Bhattacharyya et al., astro-ph/0402534 (2004).
  27. S. E. Woosley et al., *Ap. J. Suppl.* 151 (2004) 75.
  28. R. K. Wallace and S. E. Woosley, *Ap. J. Suppl.* 45 (1981) 389.
  29. L. van Wormer et al. *Ap. J.* 432 (1994) 326.
  30. H. Schatz *et al.*, *Phys. Rep.* 294 (1998) 167.
  31. H. Schatz *et al.*, *Phys. Rev. Lett.* 86 (2001) 3471.
  32. M. Wiescher and H. Schatz, *Journ. Phys. G Topical Review* 25 (1999) R133.
  33. R. N. Boyd, M. Hencheck, and B. S. Meyer, in *International Symposium on Origin of Matter and Evolution of Galaxies 97, Atami, Japan*, edited by S. Kubono, T. Kajino, K. I. Nomoto, and I. Tanihata (World Scientific, New Jersey, Singapore, 1998), p. 350.
  34. R. E. Taam, S. E. Woosley, and D. Q. Lamb, *Ap. J.* 459 (1996) 271.
  35. O. Koike *et al.*, *Astron. Astrophys.* 342 (1999) 464.
  36. H. Schatz *et al.*, *Ap. J.* 524 (1999) 1014.
  37. O. Koike et al. *Ap. J.* 603 (2004) 242.
  38. F.-K. Thielemann et al., *Prog. in Part. and Nucl. Phys.* 46 (2001) 46.
  39. J. L. Fisker, F.-K. Thielemann, and M. Wiescher, *Ap. J.* 608 (2004) 61.
  40. M. Czerny, B. Czerny, and J. E. Grindlay, *Ap. J.* 312 (1987) 122.
  41. I. Fushiki et al. *Ap. J.* 390 (1992) 634.
  42. A. Cumming, astro-ph/0309626 (2003).
  43. R. E. Taam, *Ap. J.* 241, (1980), 358
  44. D. K. Galloway et al. *Ap. J.* 601 (2004) 466.
  45. B. A. Fryxell and S. E. Woosley, *Ap. J.* 261 (1982) 332.
  46. L. Bildsten, *Ap. J.* 438 (1995) 852.
  47. A. Spitkovsky, Y. Levin, and G. Ushomirsky, *Ap. J.* 566 (2002) 1018.
  48. M. Zingale et al. astro-ph/0211336 (2002).
  49. M. Zingale et al. *Ap. J. Suppl.* 133 (2001) 195.
  50. R. Cornelisse et al. *A&A* 405 (2003), 1033.
  51. R. Narayan and J. S. Heyl, *Ap. J.* 599 (2003) 419.
  52. A. Heger, private communication (2004).
  53. M. Hencheck et al. *Nuclei in the Cosmos III, Third International Symposium on Nuclear Astrophysics*, Proceedings of the Symposium held at the National Laboratories of Gran Sasso, Assergi, L'Aquila, Italy, July 1994. New York: American Institute of Physics Press. Edited by Maurizio Busso, Claudia M. Raiteri, and Roberto Gallino.

- AIP Conference Proceedings, Vol. 327, 1995, p.331.
54. D. L. Lambert, *Astron. Astrophys. Rev.* 3 (1992) 201.
  55. M. Arnould and S. Goriely, *Phys. Rep.* 384 (2003) 1.
  56. V. Costa *et al.*, *Astron. Astrophys.* 358 (2000) L67.
  57. M. Jaeger *et al.* *Phys. Rev. Lett.* 87 (2001) 250.
  58. S. Goriely *et al.* *Astron. Astrophys.* 383 (2002) L27.
  59. N. Dauphas *et al.* *astro-ph/0211452* (2002).
  60. J. M. M. in't Zandt, R. Cornelisse, and A. Cumming, *Astron. Astrophys.* 426 (2004) 257.
  61. J. M. M. in't Zandt *et al.* *astro-ph/0407087* (2004).
  62. T. E. Strohmayer and C. B. Markwardt, *Ap. J.* 577 (2002) 337.
  63. T. E. Strohmayer and E. F. Brown, *Ap. J.* 566 (2002) 1042.
  64. A. Cumming and L. Bildsten, *Ap. J.* 559 (2001) L127.
  65. H. Schatz, L. Bildsten, and A. Cumming, *Ap. J.* 583 (2003) L90.
  66. A. Cumming and J. Macbeth, *Ap. J.* 603 (2004) L37.
  67. E. F. Brown, *Ap. J.* 614 (2004) 57.
  68. W. Chen, C. R. Shrader, and M. Livio, *Ap. J.* 491 (1997) 312.
  69. S. Campana *et al.* *A&A rev.* 8 (1998) 279.
  70. M. Colpi, U. Geppert, D. Page, and A. Possenti, *Ap. J.* **548**, L175 (2001).
  71. D. G. Yakolev, K. P. Ikenfisch, and P. Haensel, *Astron. Astrophys.* 407 (2004) 265.
  72. E. F. Brown, L. Bildsten, and R. E. Rutledge, *Ap. J.* 504 (1998) L95.
  73. R. Rutledge *et al.*, *Ap. J.* 529 (2000) 985.
  74. R. E. Rutledge *et al.*, *Ap. J.* 514 (1999) 945.
  75. R. E. Rutledge *et al.* *Ap. J.* 577 (2002) 346.
  76. R. Wijnands, *astro-ph/0405089* (2004).
  77. R. Wijnands *et al.* *Ap. J.* 606 (2004) L61.
  78. V. Urpin, U. Geppert, and D. Kononov, *M.N.R.A.S.* 295 (1998) 907.
  79. E. F. Brown and L. Bildsten, *Ap. J.* 496 (1998) 915.
  80. A. Cumming, P. Arras, and E. Zweibel, *Ap. J.* 609 (2004) 999.
  81. P. Haensel and J. L. Zdunik, *Astron. Astrophys.* 227 (1990) 431.
  82. P. Haensel and J. L. Zdunik, *Astron. Astrophys.* 229 (1990) 117.
  83. P. Haensel and J. L. Zdunik, *Astron. Astrophys.* 404 (2003) 33.
  84. L. Bildsten *Ap. J. Lett.* 501 (1998) 89.
  85. G. Ushomirsky, C. Cutler, and L. Bildsten, *Monthly Not. of the Royal Astron. Soc.* 319 (2000) 902.
  86. P. B. Jones, *astro-ph/0403400* to appear in *Phys. Rev. Lett.* (2004).
  87. A. E. Champagne and M. Wiescher, *Ann. Rev. Nucl. Part. Sci.* 42 (1992) 39.
  88. M. Wiescher, H. Schatz, and A. E. Champagne, *Phil. Trans. Royal. Soc. London* 356 (1998) 2105.
  89. T. Radon *et al.* *Phys. Rev. Lett.* 78 (1997) 4701
  90. J. Stadlmann *et al.*, *Phys. Lett.* B586 (2004) 27
  91. A. Wöhr *et al.*, *Nucl. Phys.* A742 (2004) 349
  92. M. Chartier. *et al.*, *Nucl. Phys.* A637 (1998) 3
  93. H. Stolzenberg *et al.*, *Phys. Rev. Lett.* 65 (1990) 3104
  94. G. Savard *et al.*, *Nucl. Phys.* A626 (1997) 353

95. V. S. Kolhinen et al., Nucl. Instr. Methods A528 (2004) 776
96. S. Schwarz et al. Nucl. Instr. Meth. B 204 (2003) 507
97. G. Audi, A. H. Wapstra and C. Thibault, Nucl. Phys. A 729 (2003) 129.
98. B. A. Brown, R. R. C. Clement, H. Schatz, A. Volya, W. A. Richter, Phys. Rev. C65 (2002) 045802
99. D. Lunney, J. M. Pearson, and C. Thibault, Rev. Mod. Phys. 75 (2003) 1021.
100. J. A. Clark et al., Phys. Rev. Lett. 92 (2004) 192501
101. J. A. Clark et al., Proceed. of the Fourth Internat. Conf. on Exotic Nuclei and Atomic Masses, (2004) 59
102. D. Rodriguez et al. Phys. Rev. Lett. 93 (2004) 161104
103. R. J. Tighe et al., Phys. Rev. C49 (1994) R2871
104. J. Friese et al., in Proceedings of the XXIV Workshop on Gross Properties of Nuclei, Hirschegg, Austria 1996, edited by H. Feldmeier, J. Knoll and W. Nörenberg (GSI Darmstadt 1996) p. 123
105. G.M. Fuller, W.A. Fowler and M. J. Newman, Astrop.J. 252 (1982) 715
106. J. Pruet and G. M. Fuller, Astrop. J. Suppl. 149 (2003) 189
107. T. Rauscher, F. K. Thielemann, At. Data Nucle. Data Tab. 75 (2000) 1
108. H. Herndl et al. Phys. Rev. C 52 (1995) 1078.
109. J. L. Fisker et al. Atomic Data and Nucl. Data Tab. 79 (2001) 241.
110. H. O. U. Fynbo et al. Nature 433 (2005) 136
111. P. Decrock et al., Phys. Rev. Lett. 67 (1991) 808
112. Th. Delbar et al., Phys. Rev. C48 (1993) 3088
113. S. Bishop et al., Phys. Rev. Lett. 90 (2003) 162501
114. I. Y. Lee, Nucl. Phys. A 520 (1990) 641c
115. W. F. Mueller et al., Nucl. Instr. Methods A 466 (2001) 492.
116. T. Motobayashi et al., Phys. Lett. B264 (1991) 259
117. J. Kiener et al., Nucl. Phys. A552 (1993) 66
118. C. Angulo, NACRE-Nuclear Astrophysics Compilation of Reaction Rates, <http://pntpm.ulb.ac.be/nacre/> (2003)
119. X. Tang et al., Phys. Rev. C69 (2004) 055807
120. B. Harss et al., Phys. Rev. Lett. 82 (1999) 3964
121. J.C. Blackmon et al., Nucl Phys. A688 (2001) 142
122. B. Harss et al., Phys. Rev. C65 (2002) 035803
123. J. C. Blackmon et al., Nucl. Phys. A718 (2003) 127c
124. M. Notani et al., Nucl. Phys. A746 (2004) 113c
125. D. W. Bardayan et al., Phys. Rev. Lett. 83 (1999) 45
126. D. W. Bardayan et al., Phys. Rev. C62 (2000) 055804
127. A. Galindo-Uribarri et al. Nucl. Instr. Methods B172 (2000) 647
128. W. Bradfield-Smith et al., Phys. Rev. C59 (1999) 3402
129. D. Groombridge et al., Phys. Rev. C66 (2002) 055802
130. S. Sinha et al., Bull. Am. Phys. Soc. (2004)
131. R. D. Page et al., Phys. Rev. Lett. 73 (1994) 3066
132. G. Vancraeynest et al., Phys. Rev. 57 (1998) 2711
133. M. Couder et al. Phys. Rev. C 69 (2004) 022801
134. L. O. Lamm et al., Nucl. Phys. A510 (1990) 503

- 135.S. Kubono et al., Phys. Rev. C46 (1992) 361
- 136.B. A. Brown, A. E. Champagne, H. T. Fortune and R. Sherr, Phys. Rev. C48 (1993) 1456
- 137.D. Seweryniak et al., Phys. Lett. B590 (2004) 170
- 138.R. E. Azuma et al., Nucl. Phys. A718 (2003) 199c
- 139.J. M. D'Auria et al. Phys. Rev. C69 (2004) 065803
- 140.S. Seuthe et al., Nucl. Phys. A514 (1990) 471
- 141.F. Stegmüller et al., Nucl. Phys. A601, (1996) 168
- 142.D. G. Jenkins et al., Phys. Rev. Lett.92 (2004) 031101
- 143.J. A. Caggiano et al., Phys. Rev. C64 (2001) 025802
- 144.T. Gomi et al., Nucl. Phys. A734 (2004) E77
- 145.H. Schatz et al., Phys. Rev. Lett. 79 (1997) 3845
- 146.R. R. C. Clement et al., Phys. Rev. Lett. 92 (2004) 172502
- 147.K. E. Rehm et al., Phys. Rev. Lett. 80 (1998) 676
- 148.K. E. Rehm et al., Nucl. Instr. Meth. A449 (2000) 208
- 149.C. L. Jiang et al., Argonne National Laboratory Annual Report, ANL-99/12 (1999) 11, unpublished
- 150.X. G. Zhou et al. Phys. Rev. C53 (1996) 982
- 151.O. Forstner et al. Phys. Rev. C64 (2001) 5801.
- 152.K. E. Rehm et al., Phys. Rev. C67 (2003) 065809
- 153.B. Davids et al., Phys. Rev. C67 (2003) 012801
- 154.B. Davids et al., Phys. Rev. C67 (2003) 065808
- 155.G. P. A. Berg et al., Nucl. Phys. A718, (2003) 608c
- 156.J. A. Caggiano et al., Phys. Rev. C66 (2002) 015804
- 157.N. Bateman et al., Phys. Rev. C63 (2001) 035803
- 158.D. Seweryniak et al., accepted in Phys. Rev. Lett.